Original Article

JCBFM

Journal of Cerebral Blood Flow & Metabolism
2017, Vol. 37(2) 590–604

DOI: 10.1177/0271678X16634715
jcbfm.sagepub.com

SAGE

From unspecific to adjusted, how the BOLD response in the rat hippocampus develops during consecutive stimulations

Stephanie Riemann[1], Cornelia Helbing[1] and Frank Angenstein[1,2]

Abstract

To determine the possibility to deconvolve measured BOLD responses to neuronal signals, the rat perforant pathway was electrically stimulated with 10 related stimulation protocols. All stimulation protocols were composed of low-frequency pulse sequences with superimposed high-frequency pulse bursts. Because high-frequency pulse bursts trigger only one synchronized spiking of granular cells, variations of the stimulation protocol were used: (a) to keep the spiking activity similar during the presentation of different numbers of pulses, (b) to apply identical numbers of pulses to induce different amounts of spiking activity, and (c) to concurrently vary the number of applied electrical pulses and resultant spiking activity. When complex pulse sequences enter the hippocampus, an unspecific default-like BOLD response is first generated, which relates neither to the number of incoming pulses nor to the induced spiking activity. Only during subsequent stimulations does the initial unspecific response adjust to a more adequate response, which in turn either strongly related to spiking activity when low-frequency pulses were applied or depended on the incoming activity when high-frequency pulse bursts were presented. Thus, only the development of BOLD responses during repetitive stimulations can predict the underlying neuronal activity and deconvolution analysis should not be performed during an initial stimulation period.

Keywords

Functional magnetic resonance imaging, dentate gyrus, electrophysiology, neurovascular coupling, field excitatory post-synaptic potential

Received 14 October 2015; Revised 8 January 2016; Accepted 2 February 2016

Introduction

Functional magnetic resonance imaging (fMRI) is frequently used to study functional connectivities in the brain. Because the relevant interactions take place at the neuronal level the measured BOLD-fMRI signals have to be deconvolve to neuronal activities. That means based on the measured hemodynamic parameters, a pattern of neuronal activity has to be determined, which should correlate with each other in case there is a functional connectivity between two regions. This turns out to be problematic because the relation between BOLD signal and neuronal activity is nonunique.[1–3] Variations in BOLD signal as a basis for fMRI reflect a complex hemodynamic reaction to altered neuronal activity. On the one hand, increased neuronal activity affects the local blood flow, i.e. released vasoactive factors dilate arterioles, leading to functional hyperemia; on the other hand, the increased neuronal activity requires additional energy, thus the local glucose and oxygen consumption also increases. In most cases, the increased supply of blood oxygen exceeds the actual consumption and as a consequence, the venous blood becomes more oxygenated, which in turn increases the signal intensity in a T_2^*-weighted image.[4,5] The neurophysiological

[1]Functional Neuroimaging Group, Deutsches Zentrum für neurodegenerative Erkrankungen (DZNE), Magdeburg, Germany
[2]Special Lab for Noninvasive Brain Imaging, Leibniz Institute for Neurobiology, Magdeburg, Germany

Corresponding author:
Frank Angenstein, Functional Neuroimaging Group, Deutsches Zentrum für neurodegenerative Erkrankungen (DZNE), Leipzigerstr. 44, 39118 Magdeburg, Germany.
Email: frank.angenstein@dzne.de

processes that link neuronal activity with hemodynamic responses (i.e. neurovascular coupling) have been extensively studied[6–11] and it appears that neuronal activity-dependent rather than energy metabolite-mediated mechanisms control the vascular response.[12]

In general, neuronal activity comprises synaptic (input) and spiking (output) activity, both of which could have an impact on the BOLD response formed. Both forms of neuronal activity are mutually dependent and as long as they change in the same way, stimulus-induced variations in BOLD signal intensities can be related to variations in neuronal activity.[13] Initial studies indicated a stronger relation of the BOLD response to (post)synaptic activity than to spiking activity,[9] whereas later studies, especially using optogenetic stimulation of glutamatergic neurons, instead also pointed to spiking-related mechanisms[14–16]; however, a similar approach indicated that the amount of (post)synaptic activity better related to the formed BOLD response.[17] Thus, there are evidences from optogenetic approaches and peripheral (visual) stimulations that favor synaptic activity as driving force for the formation of a BOLD response.[9,17] But there are also evidences from optogenetic approaches and peripheral (auditory) stimulations for a crucial role of spiking activity[18,19] for the formation of a BOLD response as well as evidences from optogenetic and electrical stimulation approaches that the two forms of neuronal activity control the generation of a BOLD response.[20,21]

To disentangle the contribution of each individual component to the BOLD response, an experimental approach is required that keeps one form of neuronal activity similar under one experimental condition (i.e. same animal species, form of stimulations and region of activation), while the other form is altered. In previous studies, we used electrical perforant pathway stimulation with low frequency pulse trains or high frequency burst pulses to trigger monosynaptic neuronal responses in the dentate gyrus.[22,23] This approach has the advantage that by electrical stimulation of a central fiber bundle only axons projecting directly to the hippocampus are targeted. Thus, each applied electrical pulse elicits one action potential that arrives in the dentate gyrus or other parts of the hippocampal formation. Therefore, the number of applied pulses (defined by the specific stimulation protocol) is synonymous with the incoming activity. Concurrently, the induced spiking activity of the principal neurons in the dentate gyrus, i.e. the granular cells, can be measured as population spike by extracellular field recordings. The population spike amplitude relates to the amount of synchronized spiking of the granular cells and therefore it represents the amount of output activity[24] from the dentate gyrus. That means, input activity and output activity can be related to the simultaneously measured BOLD response in the dentate gyrus. Whereas low frequency pulses trigger one population spike per incoming pulse, high frequency pulses trigger only one population spike to the first incoming pulse in most cases. Consequently, the combination of low frequency pulse stimulation (e.g. 1, 5, 10 Hz) with superimposed high-frequency pulse bursts (i.e. 2, - 20 pulses) allows the application of specific pulse patterns, in which the same number of electrical pulses (i.e. the same amount of input activity) trigger different numbers of population spikes or a different number of electrical pulses (i.e. different amount of input activity) trigger the same number of population spikes (Figure 1). Consequently, this experimental approach allows conclusions to be drawn about the impact of incoming and/or outgoing activity for the formation of a BOLD response.

Material and methods

Animals were cared for and used according to a protocol approved by the animal experiment committee, and in conformity with the European convention for the protection of vertebrate animals used for experimental purposes and institutional guidelines 86/609/CEE, 24 November 1986. The experiments were approved by the animal care committee of the State of Saxony-Anhalt (No.: 42502-2-1218 DZNE) and were performed according to the ARRIVE (Animal Research: Reporting In Vivo Experiments) guidelines. Male Wistar-Han rats were housed individually in conditions of constant temperature (23 °C) and maintained on a controlled 12:12 h light/dark cycle, with food and tap water available ad libitum. For all experiments, 119 animals (experiment 1: $n = 40$, experiment 2: $n = 33$, experiment 3: $n = 24$, experiment 4: $n = 22$) were scanned.

Surgery and electrode implantation

Nine-week-old male Wistar-Han rats (270–330 g) were deeply anesthetized with Nembutal (40 mg/kg, i.p.) and placed in a stereotactic frame. To stimulate the hippocampal formation, a bipolar stimulation electrode (114 µm in diameter, Teflon-coated tungsten wire, A-M Systems) was placed into the perforant pathway (AP: −6.9 mm; ML + 4.1 mm from Bregma; DV 2.3–3.0 mm from dural surface) of the right hemisphere, according to the atlas of Paxinos and Watson.[25] For measuring the electrophysiological response in the hippocampus, a monopolar recording electrode (AP: −2.8 mm, ML: −1.8 mm; DV: 2.9–3.5 mm from Dura) was placed in the granular cell layer of the right dentate gyrus. The correct placement of stimulation and recording electrodes during the implantation was verified by measuring monosynaptic field potentials. Silver-wire

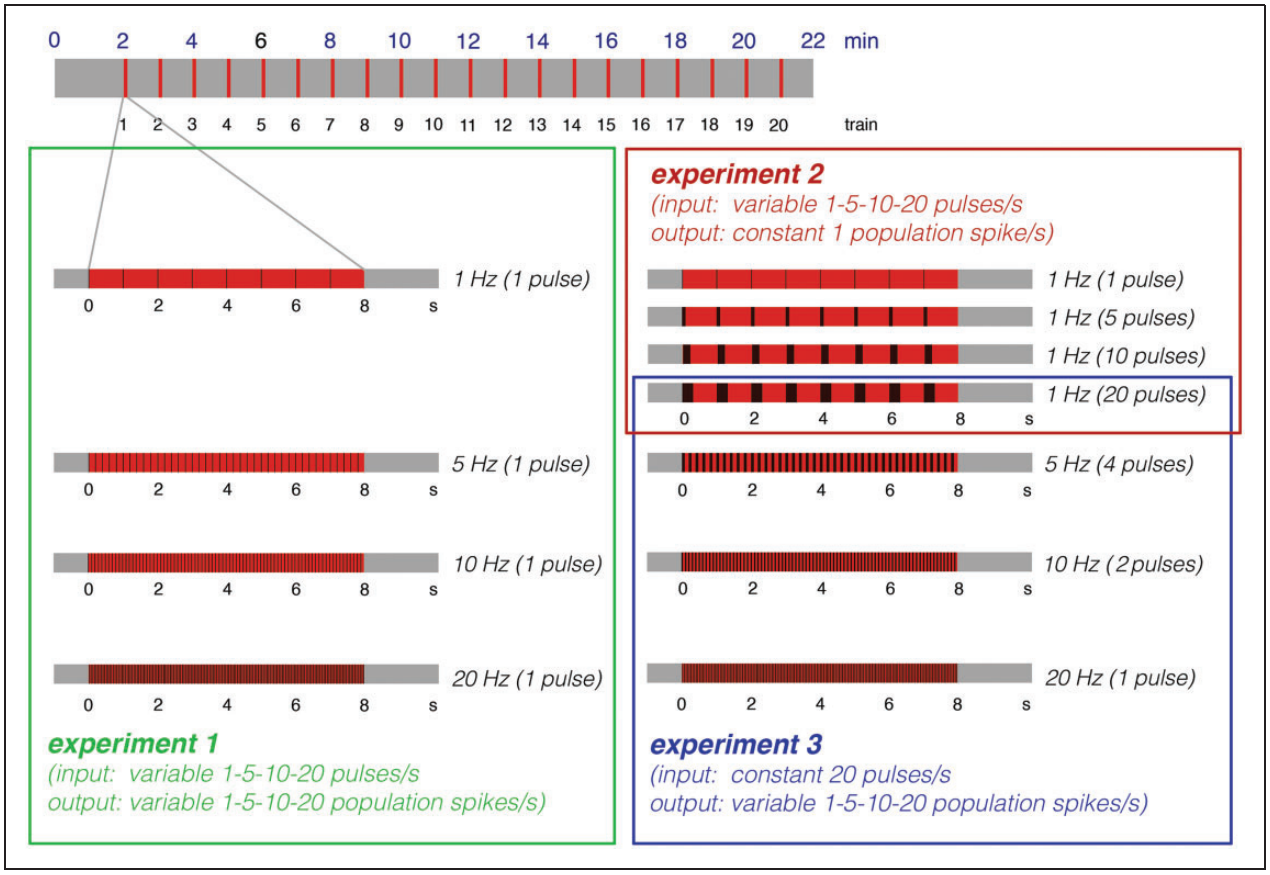

Figure 1. Summary of the applied stimulation protocols. During all experiments, the perforant pathway was stimulated with 20 consecutive stimulation trains. The first stimulation train (indicated by red boxes) was applied 2 min after starting fMRI. Each stimulation train lasts for 8 s and was followed by 52 s rest (indicated by the gray boxes). During the first set of experiments, continuous 1, 5, 10, or 20 Hz pulses were applied during each stimulation train. During these stimulation frequencies, each applied pulse elicited one population spike; consequently, under these conditions, the input (i.e. applied pulses) and output activity (number of population spikes) vary in a similar way (Experiment 1). In a second set of experiments, high frequency pulses (5, 10, or 20) were superimposed on a 1 Hz stimulation protocol. Because only one population spike was generated to the first pulse of the burst during these conditions, whereas all subsequent pulses only generated fEPSPs, the number of population spikes was similar. Consequently, only the incoming activity varied, whereas the output activity remained similar (Experiment 2). During the third set of experiments, the perforant pathway was additionally stimulated with 5 Hz-4 pulses and 10 Hz-2 pulses; thus, there were four different experimental conditions in which 20 pulses were applied but different numbers of population spikes were generated (Experiment 3).

grounding and reference electrodes were placed on the dura of the left skull and fixed with plastic screws and dental cement.

Electrical stimulation and fMRI

All combined electrophysiology/fMRI measurements were performed on a 4.7 T Bruker Biospec 47/20 animal scanner (free bore of 20 cm) equipped with a BGA09 (400 mT/m) gradient system (Bruker BioSpin GmbH, Ettlingen, Germany). A 50 mm Litzcage small animal imaging system (DotyScientific Inc., Columbus, SC, USA) was used for the RF signal reception.

All animals were initially anesthetized with isoflurane (1.5–1.8%; in 50:50 N_2:O_2; v:v) and the anesthesia was switched to deep sedation by the application of medetomidine (Dorbene, Pfizer GmbH, bolus: 50 µg/kg s.c. and after 15 min 100 µg/kg per h s.c.) after animals were fixed into the head holder and connected to recording and stimulation electrodes.

All necessary MRI and electrophysiological adjustments for the simultaneous fMRI experiment were set in parallel before the measurements began. Breathing, heart rate, and oxygen saturation were monitored throughout the experiment by an MRI-compatible pulse oximeter (MouseOX^{TM}; Starr Life Sciences Corp., Pittsburgh, PA, USA). Heating was provided from the ventral site. To determine the appropriate stimulation intensity for the fMRI experiment, the perforant pathway was first stimulated with single test

pulses (pulse duration 0.2 ms) at increasing intensities (i.e. 3 test pulses at 10 s intervals with the following intensities: 100, 200, 300, 400, 500, 600 μA; recordings were made at an interval of 2 min except for values above 400 μA, which was taken after a 4-min interval). According to this input/output curve, the stimulation intensity that elicited 50% of the maximal population spike amplitude was determined for each animal and used for the continuous stimulation protocol (i.e. the stimulation intensity was between 200 and 300 μA).

The perforant pathway was stimulated with 20 consecutive stimulation trains; the first train was presented 2 min after starting the fMRI session. Each train lasted 8 s and was followed by 52 s rest, thus at the beginning of every minute, one stimulation train was applied. The stimulation sequence for each train is summarized in Figure 1. The total scanning time for the combined fMRI-electrophysiology experiment was 22 min. The combined fMRI and electrophysiology session started 30 min after placement of the rat in the scanner, thus total time for pre-adjustments and data acquisition was less than 1 h.

The electrophysiological responses during stimulation were recorded with a sample rate of 5000 Hz, filtered between 1 and 5000 Hz by using a differential amplifier EX 4-400 (Science Products, Hofheim, Germany), transformed by an analogue-to-digital interface (power-CED, Cambridge Electronic Design, Cambridge, UK) and stored on a personal computer. No further processing filter was needed, because the minor artifacts of the imaging system were small in comparison with the recorded field potential.

For anatomical images, 10 horizontal T_2-weighted spin-echo images were obtained with a *RARE* sequence (rapid acquisition relaxation enhanced[26]) with the following parameters: TR 4000 ms, TE 15 ms, slice thickness 0.8 mm, FOV $37 \times 37\,mm^2$, matrix 256×256, RARE factor 8, and number of averages four. The total scanning time was 8 min 32 s. fMRI was performed with a gradient EPI (echo planar imaging) sequence with the following parameters: TR 2000 ms, TE 24 ms, slice thickness 0.8 mm, FOV $37 \times 37\,mm^2$, matrix 92×92, and total scanning time per frame 2 s. The slice geometry, i.e. 10 horizontal slices, was identical to the previously obtained anatomical spin-echo-images.

Data processing and analysis

The functional data were loaded and converted into BrainVoyager data format. A standard sequence of preprocessing steps implemented in the BrainVoyager QX software (Brain Innovation, Maastricht, the Netherlands), such as slice scan time correction, 3D motion correction (trilinear interpolation and reduced data using the first volume as a reference), and temporal filtering (high pass GLM-Fourier: three sines/cosines and Gaussian filter; FWHM 3 data points) were applied to each data set. Because the reconstruction of the fMRI images resulted in a 128×128 matrix (instead of the 92×92 imaging matrix), a spatial smoothing (Gaussian filter of 1.4 voxel) was added. Functional activation in each individual animal was analyzed by using the correlation of the observed BOLD signal intensity changes in each voxel with a predictor (hemodynamic response function), generated from the given stimulus protocol (see above); based on this, the appropriate activation map could be generated. To calculate the predictor, the square wave representing stimulus on and off conditions was convolved with a double gamma hemodynamic response function (onset 0 s, time to response peak 5 s, time to undershoot peak 15 s). To exclude false-positive voxels, we only considered those with a significance level (p) above the threshold set by calculating the false discovery rate (FDR) with a q-value of 0.05 (which corresponds to a t value greater than three or $p < 0.005$). The BOLD time series depicted for each region represent variations in BOLD signal intensities of all significantly activated voxels in the corresponding region of interest. The BOLD time series shown in all figures are the averages (arithmetic mean) of all BOLD signal time series measured in all individual animals ± standard deviations (SD).

Based on these BOLD time series, event-related BOLD responses were calculated by measuring the signal intensities starting six frames before stimulus onset (−12 s until 0 s), during stimulus presentation (between 0 and 8 s, which corresponds to four frames) and the following 15 frames (8 to 38 s) after the end of the stimulus (Figure 2). To avoid the confounding effect of putative variations in baseline BOLD signal intensities on the calculated BOLD response (i.e. BOLD signal $_{stimulus}$/ BOLD signal $_{baseline} \times 100\%$), each BOLD response was related to BOLD signal intensities of the stimulus over the preceding 12 s. To compare average maximal BOLD responses between conditions, a two-tailed unpaired Student's *t*-test was performed. Differences were considered significant at a calculated p-value < 0.05.

To summarize the spatial distribution of significantly activated voxels during a particular stimulation condition, all fMRI data sets were aligned to a 3D standard rat brain using anatomical landmarks. These data sets were then further analyzed with a linear regression analysis (general linear model (GLM) and multi-subject analysis implemented in BrainVoyager QX software). To provide a conservative representation of the main effects, the significance level was set to $t_{min} = 6$ ($p < 7.2 \times 10^{-9}$). All significantly activated voxels were converted into volumes of interest (VOI), from which surface clusters were created and visualized with the BrainVoyager VOI analysis tool.

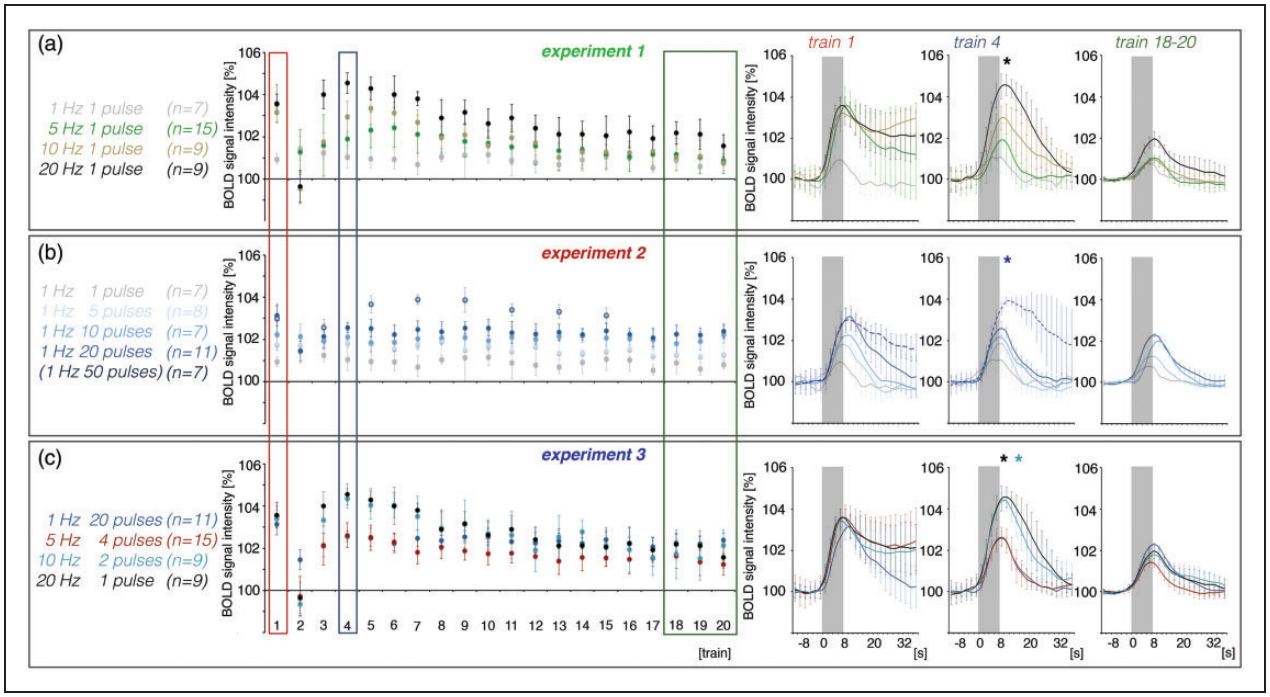

Figure 2. Summary of the measured BOLD responses in the right hippocampus during electrical stimulation of the right perforant pathway. Here, averaged maximal BOLD signal intensities during each BOLD response measured in experiment 1 (a), experiment 2 (b), and experiment 3 (c) are depicted. The averaged BOLD response during the first, fourth, and 18th–20th stimulation trains are summarized on the right. Asterisks indicate significantly increased BOLD response during train 4 when compared with train 1 (black: 20 Hz-1-pulse, dark blue: 1 Hz-50-pulse, turquoise: 10 Hz-2-pulse).

Electrophysiological data were normalized to the response to the first pulse (=1) and plotted as relative changes. To visualize the development of the responses during consecutive stimulation trains, all responses in one train were averaged (Figure S1a).

Results

To study to what degree input (i.e. synaptic) and output (i.e. spiking) activity control the resultant BOLD response in the hippocampus, three different sets of experiments were performed. During the first set of experiments (Experiment 1), four stimulation protocols were used, in which an increasing number of applied electrical pulses triggered a concurrently increased number of population spikes, i.e. input and output activities varied similarly. During a second set of experiments (Experiment 2), four related stimulation protocols were used, in which a different number of applied electrical pulses triggered the same number of population spikes, i.e. only the input activity varied whereas the number of generated population spikes remained similar. During a third set of experiments (Experiment 3), again four related stimulation protocols were compared in which the same number of applied electrical pulses triggered different numbers of population spikes, i.e. the numerical input activity was kept constant whereas the output activity varied (Figure 1).

In general, consecutive identical stimulation trains caused highly variable BOLD and electrophysiological responses (Figures 2 and 3), except for most of the 1 Hz stimulation protocols. Generally, the first stimulation train caused a substantial BOLD response that was followed by an ongoing elevated BOLD signal intensity, which in turn obscured a putative BOLD response to the second train. This elevated BOLD signal intensity coincided with the appearance of heavy neuronal afterdischarges as already observed and described earlier.[22] The individual pulses during the first stimulation train generate a very variable response pattern, i.e. the amplitudes and latencies of consecutive population spikes differed considerably (Figures 3 and S2). Thereafter, BOLD responses recovered during the following two trains and then declined continuously during all succeeding trains, but with a different rate (Figure 2). This was paralleled by the development of a repeating response pattern that remained similar after train 5 and subsequently only differed in regard to the population spike amplitude (Figures 3 and S2). Based on this general BOLD time series and related electrophysiological response patterns, the response during the first train was considered a response of the naïve

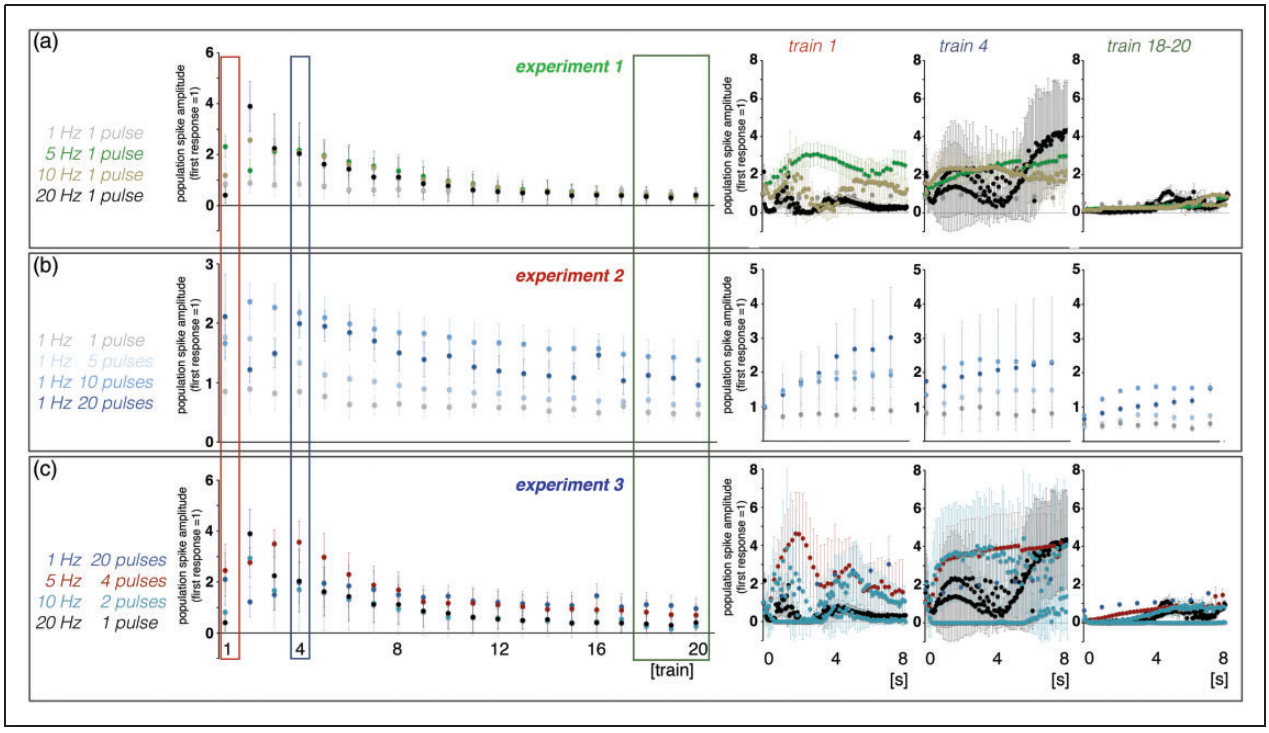

Figure 3. Summary of the electrophysiological responses in the right dentate gyrus during electrical stimulation of the right perforant pathway. Here, averaged population spike amplitudes during individual stimulus trains recorded in experiment 1 (a), experiment 2 (b), and experiment 3 (c) are depicted. The development of individual population spike amplitudes during the first, fourth, and 18th–20th stimulation trains are summarized on the right.

dentate gyrus/hippocampus to the stimulus, whereas the responses to the following three trains were considered to reflect a functional reorganization of intra-hippocampal circuitry to the incoming pulse pattern. The responses to the following trains were considered to reflect an adaptation of intra-hippocampal circuitry to these repetitive stimulations. Consequently, the response to the first stimulation train was used to compare the effect of different stimulation protocols on the resultant magnitude of the BOLD response and the last 16 trains were used to correlate variations in neuronal activity (i.e. spiking of the principal neurons) and resultant maximal BOLD responses, assuming that during this time period the general processing of the incoming activity varies only quantitatively, rather than qualitatively.

Variations in electrophysiological and BOLD responses during consecutive electrical stimulations of the perforant pathway with continuous 1, 5, 10, and 20 Hz pulse sequences (Experiment 1)

In the first set of experiments, the perforant pathway was electrically stimulated for 8 s with eight pulses (i.e. 1 Hz; n = 7), 40 pulses (i.e. 5 Hz; n = 15), 80 pulses (i.e. 10 Hz; n = 9), or 160 pulses (i.e. 20 Hz; n = 9). Because under these conditions every pulse elicited one population spike, an increase in input activity causes a concurrent increase in output activity. Consecutive continuous 1 Hz pulse stimulation trains caused almost similar BOLD responses, whereas consecutive continuous 5, 10, and 20 Hz stimulation trains caused highly variable BOLD responses, as described above (Figure 2(a)). The BOLD responses induced by the first continuous 5, 10, and 20 Hz stimulation trains were similar and significantly stronger than the BOLD response induced by the first continuous 1 Hz stimulation train. During these conditions, the first stimulation train also caused heavy after-discharges that lasted for up to 30 s, recognizable by an elevated BOLD signal intensity baseline. Thus, the formation of a BOLD response to the second stimulus train was obscured. After the third stimulation train, BOLD responses recovered and during the fourth stimulation train, the magnitudes of the BOLD response depended on the number of incoming stimuli, i.e. 5 Hz < 10 Hz < 20 Hz (Figure 2(a)). During subsequent stimulation trains, the magnitude of BOLD responses declined continuously.

Similar to the formed BOLD responses, the electrophysiologically recorded neuronal responses varied during repetitive stimulation trains. During consecutive 1 Hz stimulation trains, the average population spike amplitude per train slightly decreased during consecutive

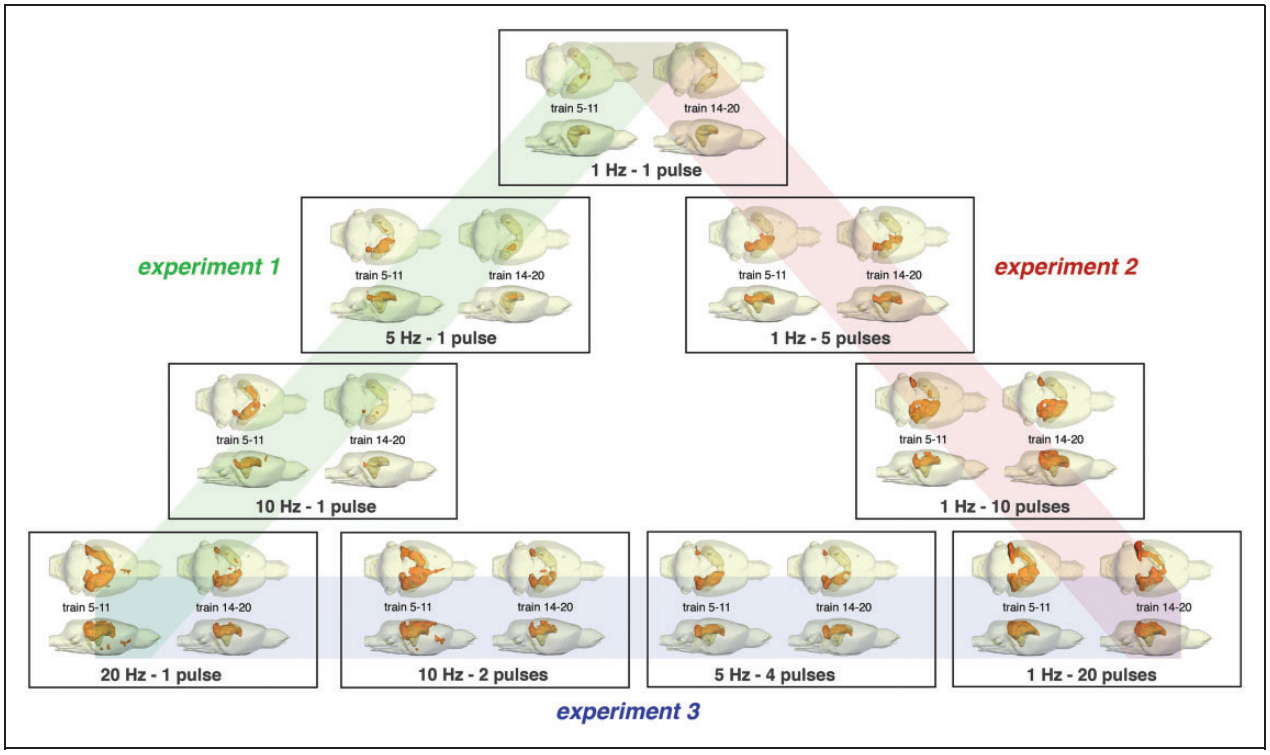

Figure 4. Distribution of significantly activated voxels depends on the actual stimulation protocol. The applied stimulation protocol does not only determine the consistency of significant BOLD responses between early (i.e. train 5–11) and late (i.e. train 14–20) trains, but also the spatial distribution.

trains, whereas the average latency per train remained almost constant (Figures 3 and S2). Within each train, the eight individual responses varied only slightly (Figure 3(a)). In contrast, average population spike amplitudes and latencies varied considerably during consecutive 5, 10, and 20 Hz stimulations. The first 5 Hz stimulation train caused an augmentation of individual responses to consecutive pulses that almost collapsed during the second train and recovered during the third. Starting with the fourth train, the average population spike amplitude declined continuously, although a steady increase of the population spike amplitude to consecutive pulses still occurred within each train. The first 10 and 20 Hz stimulation trains caused irregular spiking patterns. During the second train, stronger synchronized spiking activity of granular cells was observed which then gradually declined during all subsequent stimulation trains. Within each train, the responses increased after the first pulse.

Based on the development of summed neuronal responses during each individual train and resultant BOLD responses, strong correlations between average spiking activity and BOLD responses were found during continuous 5, 10, and 20 Hz stimulation trains, however only after functional reorganization of the hippocampal circuits, i.e. after train 4 (Figure 5).

Consecutive 1 Hz stimulation trains only induced significant BOLD responses in the dentate gyrus region of the dorsal right hippocampus (Figure 4). The spatial distribution of significant BOLD responses only declined slightly during repetitive stimulations. In contrast, consecutive 5 Hz stimulation trains caused a highly variable spatial pattern of significantly activated voxels. The early stimulation trains (i.e. trains 5–11) generated significant BOLD responses in large parts of the right hippocampus. Later, i.e. during trains 14–20, BOLD responses were only observed in a smaller area of the right hippocampus. During repetitive 10 Hz stimulations, significant BOLD responses were initially induced in large parts of the left and right hippocampus, but only in small areas of the right hippocampus during late trains. Thus, the spatial distribution of significantly activated voxels decreased considerably during repetitive stimulations. The first 20 Hz stimulation train induced initially significant BOLD responses in almost the entire right and left hippocampus, adjacent right EC, the ventral tegmental area/substantia nigra region (VTA/SN), and in the nucleus accumbens (NAcc). During late stimulations, i.e. trains 14–20, the spatial distribution of significant BOLD responses declined and no significant BOLD responses were observed outside the hippocampal formation (Figure 4).

In summary, stimulation frequencies ≥ 5 Hz generated similar BOLD responses in the hippocampus

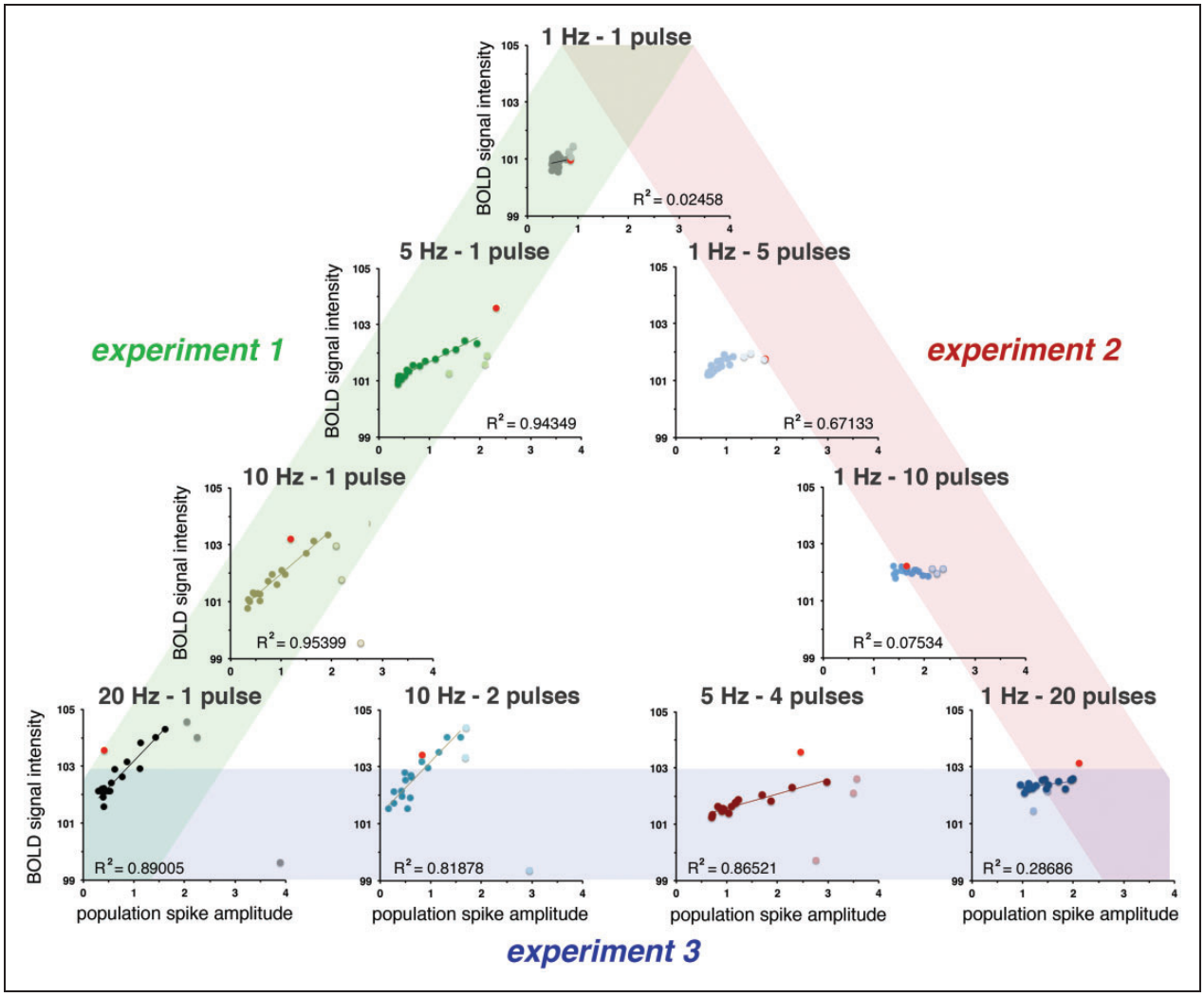

Figure 5. The relation between spiking activity (i.e. averaged population spike amplitude, see Figure 3) and the resultant BOLD response (see Figure 2) depends on the applied stimulation pattern. Strong correlations between these two factors were only found after an initial default-like BOLD response (i.e. induced by the first stimulation train, red dot) and followed by a short period of functional reconfiguration (train 2–4, pale dots). During stimulation with $\geq$ 10 high-frequency burst pulses, this correlation is nonexistent.

during the first stimulation train. Only after functional reorganization of the intra-hippocampal circuitry did the BOLD responses diverge so that stronger BOLD responses were induced with higher pulse frequencies. The spatial distribution of significantly activated voxels declined during consecutive stimulation with frequencies $\geq$ 5 Hz but remained similar during stimulation with 1 Hz.

Variations in electrophysiological and BOLD responses during consecutive electrical stimulations of the perforant pathway with different 1 Hz stimulation protocols (Experiment 2)

In the second set of experiments, high frequency pulse bursts were superimposed on a 1 Hz stimulation protocol. All of these stimulation protocols elicited only one population spike to the first pulse. Thus, the application of a single pulse (n = 7) or 5 (n = 8), 10 (n = 7), or 20 (n = 11) consecutive pulses with interpulse intervals of 10 ms caused the same number of population spikes, although the incoming activity varied by the factors of 5, 10, or 20.

The application of five pulses per burst caused significantly stronger BOLD responses than single pulses, both during the first and following all stimulation trains (Figure 2(b)). This was accompanied by the generation of a population spike with increased averaged amplitudes and reduced averaged latencies (Figures 3b and S2b). Both, the maximal BOLD responses and the average population spike amplitudes decreased slightly during consecutive trains; thus, these two factors are moderately correlated (Figure 5).

In contrast to the 1 Hz-1-pulse stimulation protocol, the spatial distribution of significant BOLD responses during stimulation of the perforant pathway with the 1 Hz-5-pulse stimulation protocol was not restricted to a small area within the right hippocampus, but extended to almost the entire right dorsal hippocampus and part of the adjacent entorhinal cortex (EC). The spatial distribution of significant BOLD responses remained almost stable during the entire experiment (Figure 4).

The application of 10 high-frequency pulses per burst generated BOLD responses with higher magnitudes during the first and following all stimulation trains than repetitive bursts with five consecutive pulses. Under this stimulation condition, the electrophysiologically recorded neuronal responses increased during the second train and then declined continuously during all subsequent stimulation trains. Because the BOLD responses remained almost constant, there was no correlation between spiking activity and the resultant BOLD response (Figures 2(b), 3(b), and 5).

The application of 20 pulses per burst again generated significantly stronger BOLD response than bursts with 10 pulses during the first and during the last 16 stimulation trains. Only during the second stimulation train the formed BOLD response was smaller (Figure 2(b)). This coincided with the appearance of neuronal after-discharges that did not occur during the other 1 Hz stimulation protocols. The 1 Hz-20-pulse protocol generated similar BOLD responses between trains 5 and 20, whereas the electrophysiologically measured responses continuously declined during this period. Consequently, no significant correlation between spiking activity and the resultant BOLD response was found under this stimulation condition (Figure 5).

Increasing the number of pulses per burst to 20 did not only cause an increased magnitude of individual BOLD responses but also a larger spatial distribution of significantly activated voxels, i.e. significant BOLD responses were also observed in the left HC and adjacent EC. Similar to the 1 Hz-5-pulse and 1 Hz-10-pulse stimulation protocols, the spatial distribution of significant BOLD responses remained almost stable during repetitive 1 Hz-20-pulse stimulations (Figure 4).

To test whether a further increase of pulses per burst causes a further increase of the generated BOLD response, the perforant pathway was also stimulated with 50 pulses per burst ($n = 7$). Because previous experiments indicated that a further increase of pulses per second may cause repetitive and heavy after-discharges,[22] the inter-train interval was extended to 112 s. This stimulation protocol initially caused the same BOLD response as stimulation of the perforant pathway with 20 pulses per burst, but after the second stimulation train, the triggered BOLD responses were significantly stronger than during the initial stimulation (Figure 2(b)).

In summary, the higher the number of pulses per burst, the higher was the magnitude of the induced BOLD response. During the first train, the maximal BOLD response was induced by bursts with 20 pulses; thus, higher numbers of pulses, e.g. 50 pulses, did not further affect the BOLD response. In contrast, after the third stimulation train, this limitation was not present. Bursts of 50 pulses caused stronger BOLD responses than during the initial first train and stronger BOLD responses than bursts with 20 trains. The spatial distribution of significantly activated voxels remained almost stable during early and late stimulation trains.

Variations in electrophysiological and BOLD responses during consecutive electrical stimulations of the perforant pathway with different 20 pulse stimulation protocols (Experiment 3)

In the first two sets of experiments, the perforant pathway was stimulated with different numbers of pulses per stimulation train. In a third set of experiments, four different stimulation protocols were compared in which the same number of pulses was applied, i.e. the perforant pathway was always stimulated with 20 pulses per second. In addition to the already described continuous 1 Hz-20-pulse and 20 Hz stimulation protocols, a 5 Hz-4-pulse ($n = 15$) and a 10 Hz-2-pulse ($n = 9$) stimulation protocol were applied. Although the same number of pulses was always applied, these protocols triggered different numbers of population spikes per second.

All four different 20 pulse stimulation protocols generated similar magnitudes of BOLD responses during the first stimulation train and the responses to the second stimulation train collapsed during all four 20 pulse stimulation protocols (Figure 2(c)). Thereupon, BOLD responses developed in a stimulus protocol-specific manner. Continuous 20 Hz and 10 Hz-2-pulse stimulation trains generated significantly stronger BOLD responses after the third train than during the first train, which then declined at a fast rate (Figure 2(c)). In contrast, maximal BOLD responses during the 1 Hz-20-pulse and 5 Hz-4-pulse protocols did not reach the initial value and were similar during the fourth train. Whereas BOLD responses during 1 Hz-20-pulse stimulation trains remained almost stable, BOLD responses during consecutive 5 Hz-4-pulse stimulations declined continuously. As a consequence of these individual developments, the strongest BOLD response during late trains was induced by the 1 Hz-20-pulse stimulation protocol.

In summary, all 20 pulse stimulation protocols initially caused the same hemodynamic response. After the third stimulation train, the BOLD responses split into two groups, i.e. similarly increased BOLD responses during 20 Hz and 10 Hz-2-pulse stimulations and similarly reduced BOLD responses during 5 Hz-4-pulse and 1 Hz-20-pulse stimulations. During subsequent stimulation trains, the maximal BOLD responses declined in a stimulus protocol-dependent manner, i.e. the higher the number of pulses per burst, the lower the decline.

Variations in electrophysiological and BOLD responses during electrical stimulations of the perforant pathway with continuous low frequency, i.e. 5 Hz, and bursts of high-frequency, i.e. 1 Hz-20-pulses, stimulation protocols (Experiment 4)

So far, the perforant pathway was stimulated with only one specific stimulation pattern. In an additional set of experiments, we tested whether the general development of BOLD responses to consecutive stimulations, i.e. fast decay during continuous low frequency stimulations and slow decay during consecutive high-frequency pulse bursts, remains present when these two forms of stimulations alternate. The perforant pathway was stimulated with ten 1 Hz-20-pulse and ten continuous 5 Hz stimulation trains. The trains were randomized and counter-balanced. Because the first stimulation trains may define the subsequent response pattern, the order was reversed in the second experiment (Figure 6). As expected, the first BOLD response was similar in the two alternating experiments, i.e. the initial 5 Hz ($n = 11$) and the 1 Hz-20-pulse ($n = 11$) stimulation protocols caused similar hemodynamic responses in the right hippocampus. The decay rate of the BOLD responses to subsequent stimulation trains was similar during the two alternate stimulation protocols and also similar for the two individual stimulation conditions (Figure 6). Consequently, during alternate stimulations, the 5 Hz stimulation protocol did not cause a strong reduction of BOLD responses during subsequent trains, as observed during solely 5 Hz stimulation trains. When the stimulation paradigm started with 5 Hz, the maximal BOLD responses of all subsequent 1 Hz-20-pulse stimulation trains were reduced. In contrast, an initial 1 Hz-20-pulse stimulation paradigm did not significantly modify subsequent BOLD responses to 5 Hz stimulation trains.

Discussion

In the present study, 10 different stimulation conditions were used to activate the hippocampal formation and measure both the induced neuronal activity in the dentate gyrus and the resultant BOLD response in the hippocampus and entire brain. The current results strengthen previous observations that the quantity and quality of neuronal activity in a given region cannot be unambiguously inferred from measured hemodynamic responses in this region.[27] This previous study already demonstrated that the same numerical amount of incoming pulses, when applied in a different pattern, can generate different BOLD responses. This study extends this finding by the observation that a similar amount of spiking activity corresponds to different BOLD responses when the causative incoming pulses differ in their pattern. Therefore, the main determinant for the formation of a BOLD response is the quality of local signal processing that sometimes relates more closely to the incoming or to the outgoing activity. Furthermore, by analyzing the spatial and qualitative developments of individual BOLD responses to consecutive stimulations, one may now draw the first conclusions about basic neurophysiological processes responsible for the observed BOLD responses. The main results of the current study are: (a) First, an unspecific nonlinear BOLD response is generated in the hippocampus when a complex pulse sequence enters the hippocampus. Only during subsequent stimulations, the initial unspecific (default-like) BOLD response will adjust to a more adequately aligned response, which then adapts, like the corresponding electrophysiological responses, during subsequent trains. Consequently, deconvolution analysis required for determining functional connectivities should not be performed during initial stimulation periods. (b) Consecutive continuous pulse trains with a frequency up to 20 Hz cause significant BOLD responses that decrease in both amplitude and spatial distribution during repetitions, whereas high-frequency burst pulse trains (inter-pulse interval 10 ms) cause BOLD responses that remain relatively stable during repetitions. Furthermore, intermittent high-frequency pulse trains lower the general decline of BOLD responses during repetitive low frequency pulse trains.

Relation between electrophysiologically measured neuronal response and resultant BOLD response

There is a long-lasting effort to relate the measured BOLD responses to the underlying neurophysiological processes. There are two basic questions: (a) What kind of neuronal activity, i.e. pre/post-synaptic activity and/or spiking activity of principal and/or interneurons, controls the measured hemodynamic response and (b) what signaling pathways mediate neurovascular coupling, i.e. what messenger molecules are released in an activity-dependent manner from neuronal and/or glia

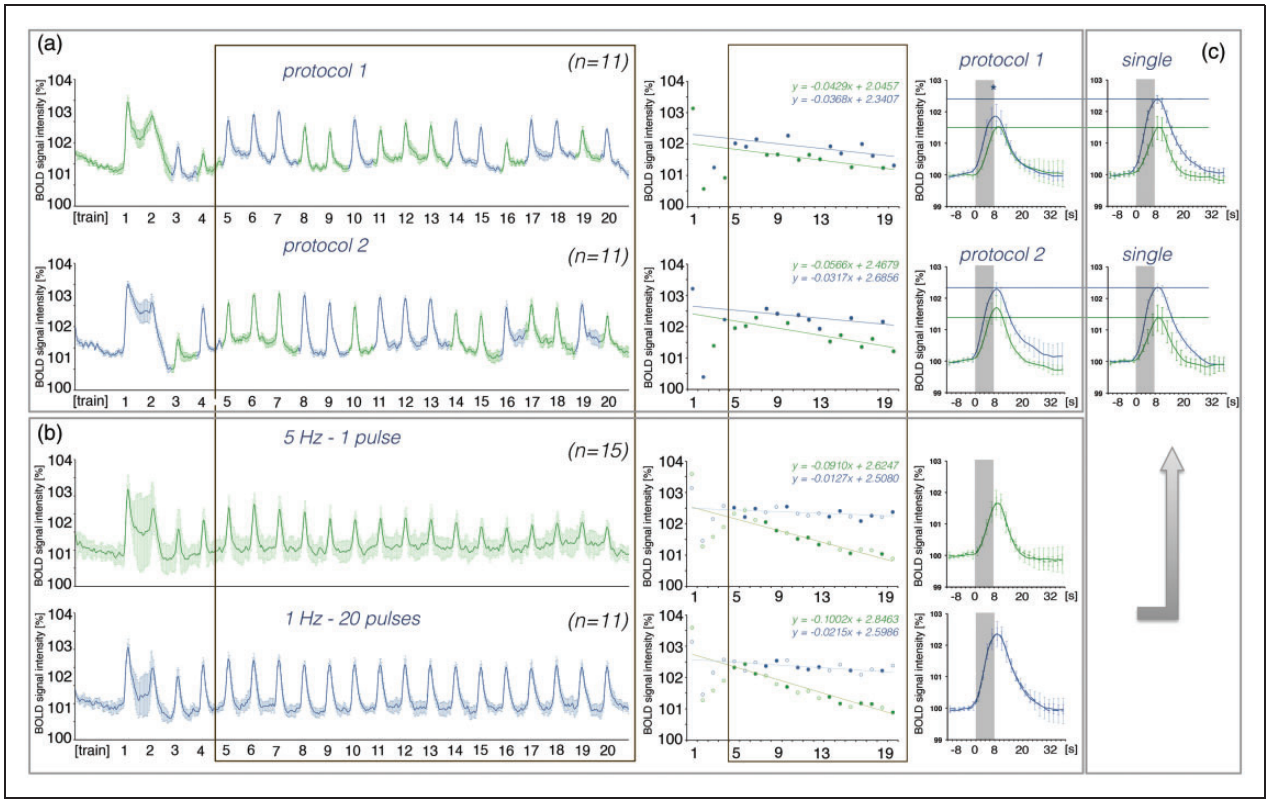

Figure 6. Application of an alternative stimulation protocol affects the development of BOLD responses to low frequency (5 Hz, green color) but not to high-frequency (1 Hz-20-pulse, blue color) stimulation. (a) Left panel: BOLD time series measured during alternate stimulations starting with a 5 Hz (protocol 1, top) or a 1 Hz-20-pulse (protocol 2, bottom) protocol. Middle panel: Summary of individual BOLD responses during stimulation and their respective decline over time (calculate between trains 5 and 20). Right panel: Averaged BOLD responses to 5 Hz and 1 Hz-20-pulse stimulation (between trains 5 and 20). (b) Left panel: BOLD time series measured during repetitive 5 Hz- and 1 Hz-20-pulse stimulations. Middle panel: Decline of BOLD responses during repetitive stimulations; top graph depicts all measuring points that correspond to protocol 1 and the lower graph depicts all measuring points that correspond to protocol 2. Right panel: average BOLD responses calculated from all responses between trains 5 and 20). (c) Comparison of BOLD responses observed during application of alternating or single stimulation protocols. An asterisk indicates a significant difference.

cells that locally modify hemodynamics. The second question is extensively studied under in vivo[28–34] and in vitro conditions,[35–40] whereas the first question can only be adequately addressed under in vivo conditions by using combined electrophysiology and fMRI. Starting with the work of the Logothetis group,[9] simultaneous extracellular recordings of field potentials and BOLD responses in the visual cortex of monkeys during peripheral stimulation became possible. Later, defined electrical stimulation of a central fiber bundle that monosynaptically projects to one brain region in which extracellular field recordings and BOLD signals were measured[41] extended the experimental setup, and recently, targeted optogenetic activation of subsets of neurons in one particular region[16,18,42,43] allowed studies of the role of specific transmitter systems for the resultant BOLD response.

To relate neurophysiological processes with hemodynamic responses, a (linear) relationship is required between at least one electrophysiologically measurable parameter and the measured BOLD response that remains present during the entire experiment, i.e. during consecutive stimulations. A previous study has already indicated that the actual excitability of the principal cells affects the prevailing mechanism for the formation of BOLD responses,[20] a result that the current study also confirms. As the intrinsic excitability may change during repetitive stimulations, a putative existing relationship between one mechanism (i.e. spiking or synaptic mediated processes) and the resultant BOLD response may become easily obscured. In addition, the current study indicates that during complex stimulations of the hippocampus, only a default-like BOLD response is initially induced that is independent of the total amount of synaptic and/or spiking activity and only after this will the BOLD response relate to the electrophysiological parameters of neuronal activities. These two confounding factors, possible changes in the

Table 1. BOLD responses and the underlying alterations in neuronal activities.

Stimulation train	Neuronal activity	BOLD response
1) **first** (initial)	• basic frequency ≤2Hz and short pulse trains (≤5 pulses) • basic frequency ≥5Hz or long pulse trains (≥10 pulses) • complex activation pattern	• *restricted to dentate gyrus* • *entire right hippocampus (i.e., dentate gyrus, CA1-CA4 and subiculum* • *default-like response*
2) **early** (between 3 and 7)	• basic frequency ≥10Hz or long pulse trains (≥50 pulses) • basic frequency <10Hz orshort pulse trains (<50 pulses)	• *magnitude of BOLD response higher than during initial train* • *magnitude of BOLD response lower than during initial train*
3) **late** (between 10 and 20)	• single pulse spike trains • bursts of high frequency pulses	• *strong decline of BOLD responses and BOLD distribution* • *moderate decline of BOLD response and almost maintained BOLD distribution*
4) between all	• no neuronal after-discharges • presence of neuronal after-discharges	• similar BOLD responses, no sustained increase in BOLD baseline intensity • collapse, followed by recovery, temporary increased BOLD signal intensity after cessation of stimuli

weighting of synaptic- or spiking-related mechanisms, as well as the switch from default to an adjusted BOLD response, can be minimized by analyzing data acquired after adjustment of the neurovascular system, i.e. after the third or fourth consecutive stimulation. This also indicates that functional connectivities based on BOLD fMRI data should not be calculated during the first stimulation period.

What defines the initial default-like BOLD response is still unclear. It is certainly not a simple ceiling effect, i.e. the maximal possible BOLD response that can be induced in this area. During several stimulation conditions (i.e. 20 Hz, 10 Hz-2-pulse, and 1 Hz-50-pulse), significantly stronger BOLD responses were induced during trains 4–7 when compared with the initial default-like response. Similarly, an unspecific hemodynamic effect, e.g. a stimulus-dependent increase in blood pressure, is not likely because no BOLD signal intensity changes were concurrently found in other brain regions. Recent work indicates that vascular responses to increased neuronal activities are largely mediated by feedforward rather than by energy-consumption-related feedback mechanisms.[10,12,38] Nevertheless, both mechanisms crucially relate on each other, in a sense that neuronal activity affects cellular cytoplasmic and mitochondrial Ca^{2+} homeostasis, which in turn dictates the existing baseline state and by that metabolic or spontaneous neural activity.[44] Thus, it is tempting to speculate that during initial stimulation, the Ca^{2+} homeostasis in neurons and glia is changed and this change persists longer than 52 s, the period between two consecutive stimulation periods. As especially astrocyte calcium signaling is crucial for neurovascular coupling,[8,45,46] any lasting changes in Ca^{2+} homeostasis should affect subsequently formed BOLD responses. Therefore, we speculate that neurovascular coupling processes differ between the first and subsequent stimulation periods. Further experiments are required to determine whether repetitive stimulations cause changes in the release of vasoactive substances from neurons and/or glia and/or whether the stimulus-induced altered intracellular Ca^{2+} concentrations in neurons and glia modifies the efficacy of neurovascular coupling processes. The latter experiments are now feasible because fMRI can be combined with measurements of intracellular Ca^{2+} concentrations.[47–49]

What can be inferred from a measured BOLD response in the hippocampus?

So far, most of the combined electrophysiological fMRI studies have been aimed at defining neurophysiological parameters that best relate to the measured hemodynamic response.[9,50–53] Of particular interest, however, would be an answer to the converse question: does the measured hemodynamic response predict specific changes in neuronal activities (other than there is an altered activity)? In the current study, we applied 10 different stimulation protocols, all using identical pulse properties, i.e. identical pulse duration and intensity. The same stimulation parameters were also used in previous studies, i.e. continuous 0.625, 1.25, 2.5 Hz stimulations,[23] continuous 100 Hz stimulations,[22] and continuous 2 Hz stimulations, paired pulse stimulations with different inter-pulse intervals.[20] Thus, an extensive

collection of data now exists relating BOLD responses in the entire hippocampal formation with the quality and quantity of incoming signals and resultant spiking activity in the dentate gyrus. Based on all of the already available data sets, it becomes obvious that one is only able to back-reference from BOLD signal changes to neuronal processes when the development of BOLD responses during consecutive stimulations is considered. This also means that averaged data (in terms of distribution and magnitude of the hemodynamic response) are of very limited significance. Table 1 lists the first general conservative conclusions about the underlying neuronal processes in the hippocampus that can be drawn from measured BOLD responses. The summarized relations between input activity and the development of formed BOLD responses in the hippocampal formation can now be used to predict the size and distribution of BOLD responses to a new stimulus pattern or as a basis for further alignment by including additional data sets.

So far, the predicting power of this approach in a more natural context, i.e. during activation of the hippocampal formation by peripheral stimuli or even during cognitive processes, is still limited by at least two factors. First, in addition to the fimbria-fornix pathway and the dorsal/ventral commissures the perforant pathway is the only one of the three major fiber bundles entering the hippocampal formation.[54] Second, all studies used artificial and very simple stimulation patterns. Already the combination of two simple stimulation patterns, i.e. continuous 5 Hz and 1 Hz-20-pulse protocols, revealed a complex interaction (Figure 6). Nevertheless, by studying more natural spike time series and/or modifications of other stimulus parameters, like pulse intensity or duration, the identified relations can easily be verified.

Electrical stimulation of CA3 pyramidal cells that project via commissural fibers to the contralateral CA1 region has been recently used to study the relation between neuronal activity and BOLD response in the hippocampus.[55] A similar approach to electrically stimulate the fimbria fornix pathway is feasible; thus, the effect of individual and combined stimulations of hippocampal afferent pathways on BOLD formation in the hippocampal formation can be determined in the future. Finally, all of these data may help to create a model to relate measured BOLD responses with basic neurophysiological processes in the hippocampal formation that can then be utilized to deconvolve BOLD signals in the hippocampus to analyze functional connectivities.

Funding

The author(s) received no financial support for the research, authorship, and/or publication of this article.

Acknowledgments

We thank K. Krautwald for her excellent technical assistance.

Declaration of conflicting interests

The author(s) declared no potential conflicts of interest with respect to the research, authorship, and/or publication of this article.

Authors' contributions

SR: data acquisition and analysis, revising manuscript, and final approval; CH: data acquisition and analysis, revising manuscript, and final approval; FA: conception and design, data acquisition and analysis, drafting manuscript, and final approval.

Supplementary material

Supplementary material for this paper can be found at http://jcbfm.sagepub.com/content/by/supplemental-data

References

1. Gitelman DR. Convolution models for fMRI. In: Toga AW (ed.) *Brainmapping, an encyclopedic reference*. Vol 1, Amsterdam: Academic Press, 2015, pp.483–488.
2. Gitelman DR, Penny WD, Ashburner J, et al. Modeling regional and psychophysiologic interactions in fMRI: the importance of hemodynamic deconvolution. *Neuroimage* 2003; 19: 200–207.
3. Zarahn E. Testing for neural responses during temporal components of trials with BOLD fMRI. *Neuroimage* 2000; 11(6 Pt 1): 783–796.
4. Ogawa S, Lee TM, Kay AR, et al. Brain magnetic resonance imaging with contrast dependent on blood oxygenation. *Proc Natl Acad Sci USA* 1990; 87: 9868–9872.
5. Ogawa S, Lee TM, Nayak AS, et al. Oxygenation-sensitive contrast in magnetic resonance image of rodent brain at high magnetic fields. *Magn Reson Med* 1990; 14: 68–78.
6. Cauli B and Hamel E. Revisiting the role of neurons in neurovascular coupling. *Front Neuroenerg* 2010; 2: 9. DOI: 10.3389/fnene.2010.00009.
7. Drake CT and Iadecola C. The role of neuronal signaling in controlling cerebral blood flow. *Brain Lang* 2007; 102: 141–152.
8. Haydon PG and Carmignoto G. Astrocyte control of synaptic transmission and neurovascular coupling. *Physiol Rev* 2006; 86: 1009–1031.
9. Logothetis NK, Pauls J, Augath M, et al. Neurophysiological investigation of the basis of the fMRI signal. *Nature* 2001; 412: 150–157.
10. Petzold GC and Murthy VN. Role of astrocytes in neurovascular coupling. *Neuron* 2011; 71: 782–797.
11. Roy CS and Sherrington CS. On the regulation of the blood-supply of the brain. *J Physiol* 1890; 11: 85–158. 17.
12. Attwell D, Buchan AM, Charpak S, et al. Glial and neuronal control of brain blood flow. *Nature* 2010; 468: 232–243.

13. Ekstrom A. How and when the fMRI BOLD signal relates to underlying neural activity: the danger in dissociation. *Brain Res Rev* 2010; 62: 233–244.
14. Kahn I, Knoblich U, Desai M, et al. Optogenetic drive of neocortical pyramidal neurons generates fMRI signals that are correlated with spiking activity. *Brain Res* 2013; 1511: 33–45.
15. Scott NA and Murphy TH. Hemodynamic responses evoked by neuronal stimulation via channelrhodopsin-2 can be independent of intracortical glutamatergic synaptic transmission. *PLoS One* 2012; 7: e29859.
16. Weitz AJ, Fang Z, Lee HJ, et al. Optogenetic fMRI reveals distinct, frequency-dependent networks recruited by dorsal and intermediate hippocampus stimulations. *Neuroimage* 2015; 107: 229–241.
17. Iordanova B, Vazquez AL, Poplawsky AJ, et al. Neural and hemodynamic responses to optogenetic and sensory stimulation in the rat somatosensory cortex. *J Cereb Blood Flow Metab* 2015; 35: 922–932.
18. Lee JH, Durand R, Gradinaru V, et al. Global and local fMRI signals driven by neurons defined optogenetically by type and wiring. *Nature* 2010; 465: 788–792.
19. Mukamel R, Gelbard H, Arieli A, et al. Coupling between neuronal firing, field potentials, and FMRI in human auditory cortex. *Science* 2005; 309: 951–954.
20. Angenstein F. The actual intrinsic excitability of granular cells determines the ruling neurovascular coupling mechanism in the rat dentate gyrus. *J Neurosci* 2014; 34: 8529–8545.
21. Kahn I, Desai M, Knoblich U, et al. Characterization of the functional MRI response temporal linearity via optical control of neocortical pyramidal neurons. *J Neurosci* 2011; 31: 15086–15091.
22. Helbing C, Werner G and Angenstein F. Variations in the temporal pattern of perforant pathway stimulation control the activity in the mesolimbic pathway. *Neuroimage* 2013; 64: 43–60.
23. Krautwald K and Angenstein F. Low frequency stimulation of the perforant pathway generates anesthesia-specific variations in neural activity and BOLD responses in the rat dentate gyrus. *J Cereb Blood Flow Metab* 2011; 32: 291–305.
24. Andersen P, Morris R, Amaral D, et al. Field potential analysis. In: Andersen P, Morris R, Amaral D, et al. (eds) *The hippocampus book*. New York, NY, USA: Oxford University Press, 2007, pp.27–30.
25. Paxinos G and Watson C. *The rat brain in stereotaxic coordinates*. San Diego: Academic Press, 1988.
26. Hennig J, Nauerth A and Friedburg H. RARE imaging: a fast imaging method for clinical MR. *Magn Reson Med* 1986; 3: 823–833.
27. Angenstein F, Kammerer E and Scheich H. The BOLD response in the rat hippocampus depends rather on local processing of signals than on the input or output activity. A combined functional MRI and electrophysiological study. *J Neurosci* 2009; 29: 2428–2439.
28. de Labra C, Rivadulla C, Espinosa N, et al. Different sources of nitric oxide mediate neurovascular coupling in the lateral geniculate nucleus of the cat. *Front Syst Neurosci* 2009; 3: 9.
29. Hall CN, Reynell C, Gesslein B, et al. Capillary pericytes regulate cerebral blood flow in health and disease. *Nature* 2014; 508: 55–60.
30. Kazama K, Anrather J, Zhou P, et al. Angiotensin II impairs neurovascular coupling in neocortex through NADPH oxidase-derived radicals. *Circ Res* 2004; 95: 1019–1026.
31. Leffler CW, Parfenova H, Fedinec AL, et al. Contributions of astrocytes and CO to pial arteriolar dilation to glutamate in newborn pigs. *Am J Physiol Heart Circ Physiol* 2006; 291: H2897–H2904.
32. Parfenova H, Tcheranova D, Basuroy S, et al. Functional role of astrocyte glutamate receptors and carbon monoxide in cerebral vasodilation response to glutamate. *Am J Physiol Heart Circ Physiol* 2012; 302: H2257–H2266.
33. Takano T, Tian GF, Peng W, et al. Astrocyte-mediated control of cerebral blood flow. *Nat Neurosci* 2006; 9: 260–267.
34. Xi Q, Tcheranova D, Basuroy S, et al. Glutamate-induced calcium signals stimulate CO production in piglet astrocytes. *Am J Physiol Heart Circ Physiol* 2011; 301: H428–H433.
35. Blanco VM, Stern JE and Filosa JA. Tone-dependent vascular responses to astrocyte-derived signals. *Am J Physiol Heart Circ Physiol* 2008; 294: H2855–H2863.
36. Cauli B, Tong XK, Rancillac A, et al. Cortical GABA interneurons in neurovascular coupling: relays for subcortical vasoactive pathways. *J Neurosci* 2004; 24: 8940–8949.
37. Dabertrand F, Hannah RM, Pearson JM, et al. Prostaglandin E2, a postulated astrocyte-derived neurovascular coupling agent, constricts rather than dilates parenchymal arterioles. *J Cereb Blood Flow Metab* 2013; 33: 479–482.
38. Filosa JA, Morrison HW, Iddings JA, et al. Beyond neurovascular coupling, role of astrocytes in the regulation of vascular tone. *Neuroscience* 2015. DOI:10.1016/j.neuroscience.2015.03.064.
39. Girouard H, Bonev AD, Hannah RM, et al. Astrocytic endfoot Ca^{2+} and BK channels determine both arteriolar dilation and constriction. *Proc Natl Acad Sci USA* 2010; 107: 3811–3816.
40. Metea MR and Newman EA. Glial cells dilate and constrict blood vessels: a mechanism of neurovascular coupling. *J Neurosci* 2006; 26: 2862–2870.
41. Angenstein F, Kammerer E, Niessen HG, et al. Frequency-dependent activation pattern in the rat hippocampus, a simultaneous electrophysiological and fMRI study. *Neuroimage* 2007; 38: 150–163.
42. Li N, van Zijl P, Thakor N, et al. Study of the spatial correlation between neuronal activity and BOLD fMRI responses evoked by sensory and channelrhodopsin-2 stimulation in the rat somatosensory cortex. *J Mol Neurosci* 2014; 53: 553–561.
43. Urban A, Rancillac A, Martinez L, et al. Deciphering the neuronal circuitry controlling local blood flow in the cerebral cortex with optogenetics in PV::Cre transgenic mice. *Front Pharmacol* 2012; 3: 105. DOI: 10.3389/fphar.2012.00105.

44. Sanganahalli BG, Herman P, Hyder F, et al. Mitochondrial calcium uptake capacity modulates neocortical excitability. *J Cereb Blood Flow Metab* 2013; 33: 1115–1126.
45. Howarth C. The contribution of astrocytes to the regulation of cerebral blood flow. *Front Neurosci* 2014; 8: 103. DOI: 10.3389/fnins.2014.00103.
46. Wang X, Takano T and Nedergaard M. Astrocytic calcium signaling: mechanism and implications for functional brain imaging. *Methods Mol Biol* 2009; 489: 93–109.
47. Sanganahalli BG, Rebello MR, Herman P, et al. Comparison of glomerular activity patterns by fMRI and wide-field calcium imaging: Implications for principles underlying odor mapping. *Neuroimage* 2015; 126: 208–218.
48. Schmid F, Wachsmuth L, Schwalm M, et al. Assessing sensory versus optogenetic network activation by combining (o)fMRI with optical Ca^{2+} recordings. *J Cereb Blood Flow Metab*, Epub ahead of print 30 November 2015. DOI: 10.1177/0271678X15619428.
49. Schulz K, Sydekum E, Krueppel R, et al. Simultaneous BOLD fMRI and fiber-optic calcium recording in rat neocortex. *Nat Meth* 2012; 9: 597–602.
50. Arthurs OJ and Boniface S. How well do we understand the neural origins of the fMRI BOLD signal? *Trends Neurosci* 2002; 25: 27–31.
51. Conner CR, Ellmore TM, Pieters TA, et al. Variability of the relationship between electrophysiology and BOLD-fMRI across cortical regions in humans. *J Neurosci* 2011; 31: 12855–12865.
52. Nir Y, Fisch L, Mukamel R, et al. Coupling between neuronal firing rate, gamma LFP, and BOLD fMRI is related to interneuronal correlations. *Curr Biol* 2007; 17: 1275–1285.
53. Shmuel A, Augath M, Oeltermann A, et al. Negative functional MRI response correlates with decreases in neuronal activity in monkey visual area V1. *Nat Neurosci* 2006; 9: 569–577.
54. Amaral D and Lavenex P. Hippocampal neuroanatomy. In: Andersen P, Morris R, Amaral D, et al. (eds) *The hippocampus book*. Oxford, New York: Oxford University Press, 2007, pp.37–114.
55. Scherf T and Angenstein F. Postsynaptic and spiking activity of pyramidal cells, the principal neurons in the rat hippocampal CA1 region, does not control the resultant BOLD response: a combined electrophysiologic and fMRI approach. *J Cereb Blood Flow Metab* 2015; 35: 565–575.